JOURNAL OF COLLOID AND INTERFACE SCIENCE 186, 447–452 (1997)
ARTICLE NO. CS964664

The Prefactor of Fractal Aggregates

CHRISTOPHER M. SORENSEN[1] AND GREGORY C. ROBERTS

Department of Physics, Kansas State University, Manhattan, Kansas 66506

Received June 21, 1996; accepted October 28, 1996

The prefactor k_0 of the fractal aggregate scaling relationship $N = k_0(R_g/a)^{D_f}$ is determined for both Diffusion Limited and Diffusion Limited Cluster Aggregation processes in spatial dimensions of 2, 3, 4, and 5. For the physically relevant case of DLCA aggregates in three dimensions we find $k_0 = 1.19 \pm 0.1$ when $D_f = 1.82 \pm 0.04$. Comparison of all aggregation types shows that the prefactor k_0 displays uniform trends with the fractal dimension D_f. Attempts to explain these trends are made based on either a common small N limit for all clusters or the packing of spheres in space.

Key Words: fractal aggregates

I. INTRODUCTION

Since the initial discovery by Forrest and Witten (1), it has become well established that random aggregates of particles formed during aggregation in colloidal or aerocolloidal systems are describable as fractals (2, 3). A consequence of this fractal morphology is that the number of monomer or primary particles N in an aggregate of size R scales as $N \propto R^{D_f}$ where D_f is the fractal dimension. Initially this proportionality was sufficient to define an aggregate or ensemble of aggregates as fractals, and it laid the foundation for this new descriptive ability. More recently it has been useful to define the size quantitatively usually as the radius of gyration R_g and to replace the proportionality with

$$N = k_0(R_g/a)^{D_f} \qquad [1]$$

where a is the monomer radius used to normalize R_g, and the proportionality constant k_0 is the prefactor of the fractal scaling relationship. Subsequent to the realization of the importance of D_f, there has been an increasing awareness that k_0 is also important for a quantitative description of aggregates (4–11). This has arisen from optical studies which show that knowledge of k_0 is important for nonintrusive light scattering measurements of soot clusters in flames and for describing their radiative properties.

The original motivation for this work was to determine k_0 for simulated, three-dimensional, DLCA aggregates which are relevant to aggregates found in nature. This has been accomplished, and we report this result, which agrees well with our experimental work (7). However, comparison of aggregates simulated by various aggregation algorithms representing different physical situations has led us to develop the idea that k_0 has more than practical value. As sure as the fractal concept and the quantifiable fractal dimension are fundamental descriptions of the aggregate morphology, so too, we believe, is the prefactor k_0. Here we present the evidence by which we have developed this belief. We have computer synthesized random aggregates using both the Diffusion Limited Aggregation (DLA) and Diffusion Limited Cluster Aggregation (DLCA) methods in a variety of spatial dimensions. Ensembles of these clusters have been fit to Eq. [1] to yield D_f and k_0. We observe empirical correlations between k_0 and D_f which we are able to describe in two different ways. The first way is to consider the small N limit of the ensemble; the second, which we believe is of greater fundamental significance, is to view k_0 as related to a packing fraction in D_f dimensional space. Our approach is empirical, and although we offer speculations concerning the meaning and implications of the observed correlations, we cannot at this time offer the fundamental reasons why these correlations work.

II. COMPUTATIONAL METHODS

Clusters were created on the computer for spatial dimensions of $d = 2$, 3, 4, and 5 for both DLA, particle-cluster, and DLCA (except $d = 5$), cluster-cluster, aggregation. In many cases we also simulated aggregation both off and on a square lattice and used different algorithms to create an isotropic aggregation. For the most part the number of monomers per cluster was kept in the range $10 \leqslant N \leqslant 100$ because our initial motivation was to create clusters similar to soot clusters which typically lie in this range (4, 5, 9–11). Although this allows the creation of fractal aggregates, our aggregates did not yield asymptotic ($N \to \infty$) values for D_f especially when $d = 4$ and 5.

The clusters were generated on an IBM PC 486 personal computer. The algorithms were written following the de-

[1] To whom correspondence should be addressed.

0021-9797/97 $25.00

scriptions in the literature (12, 13). All aggregation runs began with a list of N' monomers. Monomers during lattice simulations were considered joined when they occupied adjacent square lattice points 2a apart. During off lattice simulations, monomers joined when they were 2a apart. The sticking probability was 100%.

For DLA, one monomer was placed fixed at the center of the d-dimensional sphere and the other monomers were then introduced one by one at the starting radius at a random angular position. The starting radius was five lattice units beyond the perimeter of the central cluster. The monomer was allowed to random walk until it either joined the cluster at the center or went out of the stopping radius. The stopping radius was three times the starting radius.

For DLCA, two monomers were initially chosen from the list of N'. One monomer was fixed at the center, and the other was introduced on the starting radius as previously. The monomer then random walked until it joined the monomer at the center or went beyond the stopping radius. If the two monomers joined, the new cluster was placed back in the list which, after the first iteration, was $N' - 1$ long. If the monomer went out of the stopping radius, the attempt was aborted, and the process was repeated. Subsequent iterations involve picking two clusters at random from the list and performing the random walk again. We explored both stopping this process at some arbitrary point, "stop list," and then using the clusters so created for analysis with Eq. [1], and allowing the process to continue until only one cluster remained, "forced." No significant differences in D_f and k_0 where observed between these two methods.

For any given "type" of aggregation described by d (DLA or DLCA, stop list or forced, on or off lattice), we made 10 runs in which usually 90 clusters in the range $10 \leq N \leq 100$ were created. R_g was calculated for each cluster and N versus R_g was fit to Eq. [1]. An example of N versus R_g for one of the many cases is given in Fig. 1.

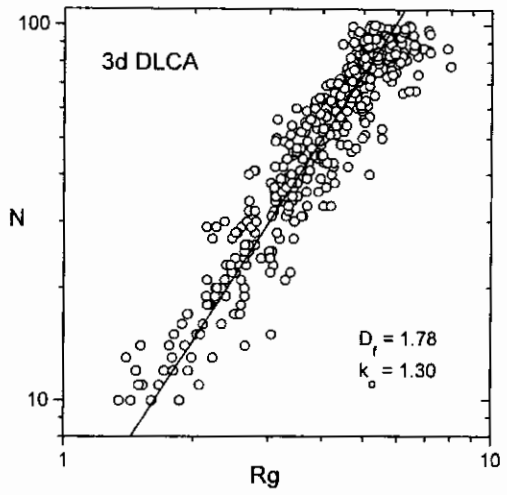

FIG. 1. An example of N versus R_g for an ensemble of clusters created by a three-dimensional DLCA simulation. The units of R_g are such that the monomer radius is $a = \frac{1}{2}$. The solid line is a best fit to Eq. [1] with fit parameters given in the figure.

III. RESULTS

For a given aggregation type the different ensembles of particles yielded different values of k_0 and D_f when fit to Eq. [1]. These different values of k_0 and D_f are just the statistical uncertainties or fluctuations from the average, and they are anticorrelated due to the nature of Eq. [1]. An example is given in Fig. 2. The source of this anticorrelation is readily apparent in Eq. [1]. For a given value of N and R_g/a, k_0 is a function of D_f. The behavior in Fig. 2 can be simply understood and quantified if one uses geometric averages of N and R_g/a for this ensemble which are $\langle N \rangle = 32$ and $\langle R_g/a \rangle = 6.1$. Use of Eq. [1] with these values yields the differential equation $dk_0 \simeq -2.2\, dD_f$ for the small region in $k_0 - D$ space near the average $k_0 = 1.27$ and $D_f = 1.80$ of Fig. 2. This quantitatively describes the anticorrelation seen in Fig. 2.

The results of the simulations are given in Table 1 where averages of D_f and k_0 are given. Also given are average D_f values from previous work (13–16) for asymptotically large, $N \to \infty$, aggregates. Disagreement between our D_f values and these literature values for $d = 4$ and 5 is due to the nonasymptotic, finite size nature of our ensembles. Despite this, two empirical observations can be made. First, in general, k_0 is anticorrelated with D_f as one compares aggregation types similar to, but of different origin than, the anticorrelation among ensembles within one aggregation type discussed previously. Second, on and off lattice aggregation yields slightly different morphologies as identified by both D_f and k_0. This different morphology as identified by D_f only has been previously observed (13), and, given the simple anticorrelation between k_0 and D_f as seen in Fig. 2, it is not surprising that k_0 differs as well. However, the difference in k_0 for on lattice and k_0 for off lattice is greater than that which can be calculated from Eq. [1] using the geometric averages of N and R_g/a as described previously for the ensembles involved. That is, if one D_f value was forced to be equal to the other, the corresponding k_0 value change prescribed by this anticorrelation would not be enough to cause the two k_0 values to be equal. Thus k_0 depends on lattice type and is not a universal quantity. This is an indication that k_0 is describing something in the morphology of the cluster beyond that describable by D_f.

IV. THE MEANING OF k_0

Figure 3 plots the results in Table 1 as k_0 versus D_f. An anticorrelation between k_0 and D_f is shown as the type of aggregation changes. This anticorrelation is weaker than that observed among ensembles of one aggregation type, shown

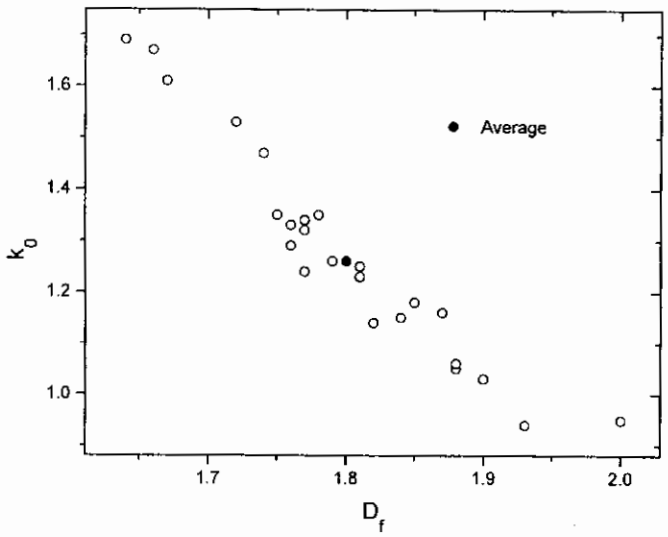

FIG. 2. The prefactor k_0 versus fractal dimension D_f for 24 different ensembles of clusters all created by a three-dimensional DLCA simulation.

in Fig. 2, and has, we believe, a different explanation. It is interesting that DLA and DLCA almost lie on the same general trend and in this context do not appear as different as they are usually described. This trend is our empirical result. Next we propose two ways of explaining the trend in k_0 versus D_f, and with these attempts begin to divine the meaning of k_0.

A. *Small N Limit*

Fractals are clusters of many monomers but consideration of plots such as Fig. 1 begs the question, what happens as $N \to 1$? Here we will argue that Eq. [1] should have the "correct" small N limit and attempt to determine what is meant by "correct." We are not trying to determine how Eq. [1] behaves at small N, which would involve corrections to the scaling of Eq. [1], but rather whether the large N behavior for all aggregation types can be governed by the same small N extrapolation. To do this we calculate R_g for clusters of small N and known geometry, use Eq. [1] to calculate k_0, and then compare to the results in Fig. 3.

Solve Eq. [1] for k_0 and then consider $N = 1$, 2, 3, and 4 in turn. The radius of gyration of a single d-dimensional sphere of radius a is

$$R_g = (d/d + 2)^{1/2}a. \qquad [2]$$

Thus for $N = 1$, Eqs. [1] and [2] yield

$$k_0(1) = \left(\frac{d+2}{d}\right)^{D_f/2}. \qquad [3]$$

For $N \geq 2$, R_g of the cluster is related to R_g of the single, d-dimension spheres and the R_g of their center points via

$$R^2_{g,\text{cluster}} = R^2_{g,\text{centers}} + R^2_{g,\text{sphere}}. \qquad [4]$$

For $N = 2$ each sphere center is its radius a from the center of mass of the dimer (the point of contact) thus $R^2_{g,\text{centers}} = a^2$. Then Eqs. [1], [2], and [4] yield

$$k_0(2) = 2\left(\frac{d+2}{2d+2}\right)^{D_f/2}. \qquad [5]$$

For $N = 3$ there are two limiting arrangements, a linear rod and an equilateral triangle for which similar arguments yield

$$k_0(3, \text{rod}) = 3\left(\frac{3d+6}{11d+16}\right)^{D_f/2}, \qquad [6]$$

$$k_0(3, \text{triangle}) = 3\left(\frac{3d+6}{7d+8}\right)^{D_f/2}. \qquad [7]$$

For $N = 4$ many configurations are possible so we consider only a simple, linear rod

$$k_0(4, \text{rod}) = 4\left(\frac{d+2}{6d+10}\right)^{D_f/2}. \qquad [8]$$

These small N limits are plotted with the data in Fig. 3. The $N = 1$ limit does not describe the data in either magnitude or the anticorrelation. The $N = 2$ limit misses in magnitude. The $N = 3$ triangle (not shown in Fig. 3) yields k_0 too big, and the $N = 4$ rod yields k_0 too small. The $N = 3$ rod, however, does an adequate job of correlating the data,

TABLE 1

Average Values of the Fractal Dimension D_f and Prefactor k_0 for the Different Types of Aggregations Simulated in This Work

d	Aggregation method	Asymptotic D_f	D_f	k_0	Symmetrized k_0
2	DLCA on lattice	1.42 ± 0.03	1.47	1.45	1.82
2	DLCA off lattice	1.46 ± 0.04	1.48	1.33	1.67
2	DLA on lattice		1.66	1.18	
2	DLA off lattice	1.71	1.66	1.08	
3	DLCA on lattice	1.78 ± 0.05	1.80	1.27	1.88
3	DLCA off lattice	1.82 ± 0.10	1.84	1.10	1.63
3	DLA on lattice		2.22	0.80	
3	DLA off lattice	2.50	2.29	0.68	
4	DLCA on lattice	2.02 ± 0.06	2.13	0.92	
4	DLA on lattice	3.40	2.78	0.54	
5	DLA on lattice		3.24	0.39	

Uncertainties in D_f and k_0 are 3% and 12%, respectively. d is the spatial dimension. Asymptotic D_f values were obtained from (13–16).

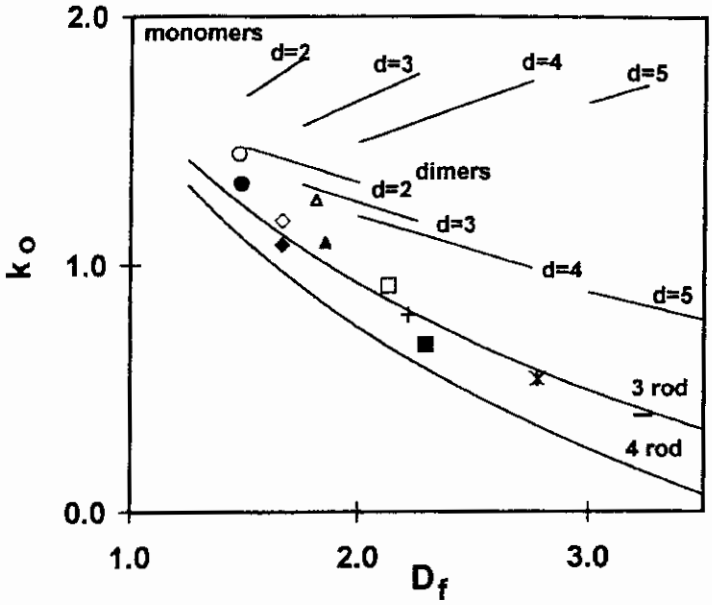

FIG. 3. The prefactor k_0 versus the fractal dimension D_f for the various aggregation types of Table 1 which are: circle, $d = 2$ DLCA; diamond, $d = 2$ DLA; triangle, $d = 3$ DLCA; square, $d = 3$ DLA; plus, $d = 4$ DLCA; plus/cross, $d = 4$ DLA; bar, $d = 5$ DLA; open symbols, on-lattice; solid symbols, off-lattice; d = spatial dimension. The labeled lines are calculated from small cluster limits described in the text as monomers, $N = 1$ limit, Eq. [3]; dimers, $N = 2$ limit, Eq. [5]; 3 rod, $N = 3$ linear rod limit, Eq. [6]; 4 rod, $N = 4$ linear rod limit, Eq. [8].

especially the DLA data. Thus one might conclude that the k_0 of fractal clusters has a value so that Eq. [1] has the correct $N = 3$ limit and that limit is a linear arrangement of three monomers. Perhaps other small N configurations could yield a comparison to the data as good as the $N = 3$ rod, but the uniqueness of this configuration is not important. The important point is that all the data, including two different aggregation schemes and four different spatial dimensions, are related in a manner that suggests that k_0 and D_f are anticorrelated through the small N limit.

The $N = 3$, linear arrangement correlation establishes a useful reference line. The DLA data tend to fall along it, whereas the DLCA data are slightly above but form a trend parallel to it. Thus from this purely empirical point of view, we have a new means of distinguishing DLA and DLCA, which is that for a given D_f, k_0 (DLCA) $> k_0$ (DLA). This combined with Eq. [1] implies a larger N in DLCA clusters than in DLA clusters of the same size, R_g/a, and same fractal dimension D_f. Later we will show that the asymmetry of DLCA clusters makes k_0 low, and a correction will be made to find a symmetrized k_0 which is larger yet.) From this perspective, *for a given* D_f, DLCA clusters are denser! This is contrary to the usual view of these two classes which concludes DLCA is the less dense because D_f is smaller for *given* d. Both views are correct; its a matter of perspective.

B. Comparison to Compact Clusters

We can use k_0 as defined in Eq. [1] and calculate its value for systems of spheres packed into clusters of integer dimension. If R is the radius of the d-dimensional, spherically symmetric cluster of monomers of radius a, then

$$N = p(d)(R/a)^d, \qquad [9]$$

where $p(d)$ is the sphere packing fraction which is a function of d and the type of packing. Combining Eqs. [1] and [2] yields

$$k_0 = p(d)\left(\frac{d+2}{d}\right)^{d/2}. \qquad [10]$$

At this time we have no *a priori* method to generalize Eq. [10] to fractal clusters of noninteger dimension D_f, but some reasonable guesses can be made and compared to the data. Equation [2] is correct for fractal clusters if d is replaced by D_f. Equation [9] can be generalized to

$$N = p(d)(R/a)^{D_f}. \qquad [11]$$

This accounts for the characteristic fractal behavior $N \sim R^{D_f}$ but retains the concept that the monomers are packed in real space of integer dimension d. Combining Eqs. [1], [2] with $d = D_f$, and [11] yields

$$k_0 = p(d)\left(\frac{D_f+2}{D_f}\right)^{D_f/2}. \qquad [12]$$

The packing fraction depends on lattice type, and three common types will be considered here:

$$\text{simple cubic, } p(d) = \frac{\pi^{d/2}}{2^d \Gamma(1 + d/2)}; \quad [13]$$

$$\text{body center cubic, } p(d) = \left(\frac{d\pi}{16}\right)^{d/2} \frac{2}{\Gamma(1 + d/2)}; \quad [14]$$

$$\text{hexagonal close pack, } p(d) = \pi/\sqrt{6d}, \quad \text{for } d = 2 \text{ or } 3. \quad [15]$$

In the above Γ is the Gamma function. Under these assumptions k_0 can now be calculated. Note that k_0 is a function of both the spatial dimension d and the fractal dimension D_f as well as the type of packing. For any given d and packing, Eq. [12] yields a k_0 which increases with D_f. This is not the trend in the data of Table 1, displayed in Fig. 3, so we will try something else.

Equation [12] can be modified to work quite well by generalizing the concept of packing to noninteger dimension. That is, in an ad hoc manner, replace $p(d)$ with $p(D_f)$ and rewrite Eq. [12] as

$$k_0 = p(D_f)\left(\frac{D_f + 2}{D_f}\right)^{D_f/2}. \quad [16]$$

For the three lattice types of Eqs. [13]–[15], Eq. [16] yields the empirical anticorrelation between k_0 and D_f found in the data. Furthermore, a reasonable comparison to the data can be obtained if the results in Table 1 are symmetrized.

The need to consider symmetry arises because Eq. [16] was derived under the assumption of a spherically symmetric cluster, whereas real clusters, especially DCLA clusters, including those formed on the computer, may be anisotropic. Qualitative consideration of Eq. [1] indicates that for fixed N, R_g would increase with increasing anisotropy (recall that R_g is a root mean square of monomer positions relative to the center of mass). Thus k_0 decreases with increasing anisotropy. To compare the data to Eq. [16] we must account for cluster anisotropy.

We assume that the perimeter of fractal cluster can be described by an ellipsoid. Let R_i, $i = 1, 2, \ldots, d$, be the axes of the ellipsoid, and $R_{g,i}$ the principal radii of gyration. Then one can show

$$R_g^2 = \sum_{i=1}^{d} R_{g,i}^2 \quad [17]$$

$$= \frac{1}{d + 2} \sum_{i=1}^{d} R_i^2. \quad [18]$$

The eccentricities are defined by

$$e_i = R_i/R_1 = R_{g,i}/R_{g,1}. \quad [19]$$

Note that $e_1 = 1$. Finally the volume is proportional to the product of the axes

$$V \propto \prod_{i=1}^{d} R_i. \quad [20]$$

The problem is, given k_0 and the eccentricities e_i of a fractal cluster, what is k_0 for a symmetric cluster of the same volume (i.e., same N)? To answer this, use Eqs. [18] and [19] to write

$$R_g^2 = \frac{R_1^2}{d + 2} \sum_{i=1}^{d} e_i. \quad [21]$$

Now find R_g of the same volume symmetric sphere as

$$R_{g,\text{sym}}^2 = \frac{d}{d + 2} R_{\text{sym}}^2, \quad [22]$$

where

$$R_{\text{sym}}^2 = \prod_{i=1}^{d} R_i \quad [23]$$

$$= R_1^d \prod_{i=1}^{d} e_i \quad [24]$$

By Eq. [1], the ratio of $(R_g/R_{g,\text{sym}})^{D_f}$ is equal to the ratio $k_{0,\text{sym}}/k_0$, thus using [21], [22], and [24] we find

$$k_{0,\text{sym}} = k_0 \left[\frac{\sum_{i=1}^{d} e_i}{d(\prod_{i=1}^{d} e_i)^{2/d}}\right]^{D_f/2}. \quad [25]$$

Given the e_i, Eq. [25] can be used to symmetrize k_0 values for anisotropic clusters.

Botet and Jullien (17) have measured the eccentricities of $d = 2$ and 3 DLCA clusters. Using their values, we calculate the correction factor in Eq. [25] to be 1.26 and 1.48 for $d = 2$ and 3, respectively. The $k_{0,\text{sym}}$ values are included in Table 1 and plotted in Fig. 4. Also graphed in Fig. 4 are k_0 values calculated for symmetric clusters with the three packing fractions, simple cubic (sc), body centered cubic (bcc), and hexagonal close packed (hcp) using Eqs. [13]–[16].

The comparison shows that the analysis does a nice job of describing the limited data. An unabashed conclusion is that DLCA clusters in $d = 2$ and 3 space pack as either body centered cubic when formed off lattice or hexagonal closed packed when formed on lattice. Furthermore, the packing densities are for noninteger dimensions D_f. Such a conclusion is tempting but needs more work to make firm.

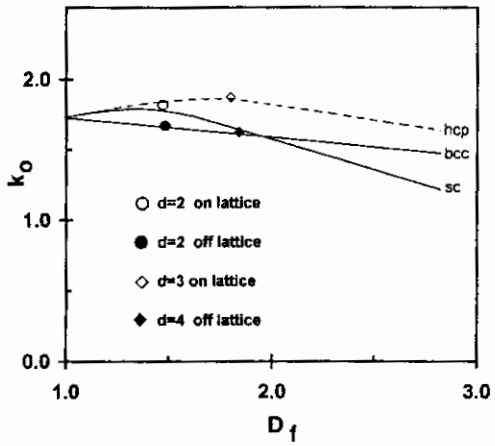

FIG. 4. The prefactor k_0 versus the fractal dimension D_f calculated as described in the text for three lattice types in a D_f dimension space. The hcp curve is dashed because it could only be calculated at $D_f = 1$, 2, and 3. Also shown are the symmetrized cluster k_0 values for DLCA clusters.

Also, it is surprising that it is the off lattice aggregation that leads to bcc packing not the on lattice; this is a surprise for which we have no explanation.

We have not determined the asymmetries of the DLA clusters. Off lattice, asymptotic DLA clusters are expected to be symmetric. Our DLA clusters are not asymptotically large; hence, a small anisotropy might exist, and this when corrected for would increase k_0 slightly. It appears, however, that this correction would not be large enough to allow Eq. [16] to agree with the data for DLA clusters.

IV. CONCLUSIONS

For $d = 3$, DLCA-simulated aggregates, we obtain $D_f = 1.82 \pm 0.04$ and $k_0 = 1.19 \pm 0.1$ when averaging our on and off lattice simulations. This is in excellent agreement with our measurements on soot for which we obtained $D_f = 1.74 \pm 0.04$ and $k_0 = 1.23 \pm 0.07$ (7), especially in light of the anticorrelation between k_0 and D_f. These values agree with the qualitative conclusions of Wu and Friedlander (6) but are significantly smaller than values on the order of $k_0 = 2.0$ to 2.4 reported by Koylu, Faeth, and coworkers (9–11).

The prefactor k_0 displays a uniform trend with the fractal dimension D_f for clusters created by either DLA or DLCA processes in a variety of spatial dimensions. The simplest explanation of this trend is that all types of clusters appear to have essentially the same small N limit regardless of aggregation type. This is reasonable since when N is small (e.g., $N = 3$), the ways in which the monomers can assemble is limited and hence is not influenced by aggregation scheme or spatial dimension.

Evidence that k_0 is related to packing of spheres into space was also presented with modest success. More work needs to be done here including creation of larger, more asymptotic clusters and calculation of anisotropies. Also the parameter R_g is imperfect here because it is not only related to the volume, hence packing fraction, of the cluster but also the distribution of monomers within the cluster. Future work will be applied in this direction.

ACKNOWLEDGMENTS

We have benefited from discussion Dr. C. Oh. This work was supported by NSF Grant CTS9408153.

REFERENCES

1. Forrest, S. R., and Witten, T. A., *J. Phys. A* **12,** L109 (1979).
2. "Kinetics of Aggregation and Gelation" (F. Family and D. P. Landau, Eds.). North Holland, Amsterdam, 1984.
3. "On Growth and Form" (N. Ostrowski and H. E. Stanley, Eds.). Nijhoff, Boston, 1986.
4. Sorensen, C. M., Cai, J., and Lu, N., *Appl. Opt.* **31,** 6547 (1992).
5. Sorensen, C. M., Cai, J., and Lu, N., *Langmuir* **9,** 2861 (1993).
6. Wu, M. K., and Friedlander, S. K., *J. Colloid Interface Sci.* **159,** 246 (1993).
7. Cai, J., Lu, N., and Sorensen, C. M., *J. Colloid Interface Sci.* **171,** 470 (1995).
8. Nyeki, S., and Colbeck, I., *J. Aerosol Sci.* **25,** 5403 (1994).
9. Koylu, U. O., and Faeth, G. M., *Comb. Flame* **89,** 140 (1992).
10. Koylu, U. O., Faeth, G. M., Farias, T. L., and Carvalho, M. G., *Comb. Flame* **100,** 621 (1995).
11. Koylu, O. U., and Faeth, G. M., *J. Heat Transfer* **116,** 152 (1994).
12. Meakin, P., *J. Colloid Interface Sci.* **102,** 491 (1984).
13. Meakin, P., *Phys. Let. A* **107,** 269 (1985).
14. Jullien, R., Kolb, M., and Botet, R., *J. Physique Lett.* **45,** L211 (1984).
15. Jullien, R., *Contemp. Phys.* **28,** 477 (1987).
16. Meakin, P., *in* "Random Fluctuations and Pattern Growth" (H. E. Stanley and N. Ostrowski, Eds.). Kluwer, Dordrecht, 1977.
17. Botet, R., and Jullien, R., *J. Phys. A* **19,** L907 (1986).